AgRISTARS

EW-L2-04387
JSC-18589

Early Warning and Crop Condition Assessment

A Joint Program for Agriculture and Resources Inventory Surveys Through Aerospace Remote Sensing

January 1983

ATMOSPHERIC EFFECTS ON METSAT DATA

W. R. Johnson

Lockheed Engineering and Management Services Company, Inc.

Earth Resources Applications Division
Lyndon B. Johnson Space Center
Houston, Texas 77058

1. Report No.	2. Government Accession No.	3. Recipient's Catalog No.
EW-L2-04387; JSC-18589		

4. Title and Subtitle	5. Report Date
Atmospheric Effects on Metsat Data	January 1983
	6. Performing Organization Code

7. Author(s)	8. Performing Organization Report No.
W. R. Johnson Lockheed Engineering and Management Services Co., Inc.	LEMSCO-18836
	10. Work Unit No.

9. Performing Organization Name and Address	11. Contract or Grant No.
Lockheed Engineering and Management Services Co., Inc. 1830 NASA Rd. 1 Houston, Texas 77058	NAS 9-15800
	13. Type of Report and Period Covered
12. Sponsoring Agency Name and Address Early Warning/Crop Condition Assessment Project Office U.S. Department of Agriculture 1050 Bay Area Blvd., Houston, Texas 77058 Technical Monitor: V. S. Whitehead	Technical Report
	14. Sponsoring Agency Code

15. Supplementary Notes

The Agriculture and Resources Inventory Surveys Through Aerospace Remote Sensing is a joint program of the U.S. Department of Agriculture, the National Aeronautics and Space Administration, the National Oceanic and Atmospheric Administration (U.S. Department of Commerce), the Agency for International Development (U.S. Department of State), and the U.S. Department of the Interior.

16. Abstract

When using the J. V. Dave dataset, two channels of simulated Metsat advanced very high resolution radiometer (AVHRR) data compare favorably with actual data. Simulated NOAA6 and NOAA7 AVHRR data are presented as radiance profiles of reflected solar energy through atmospheres with three different aerosol levels. Effects of the atmosphere on the data are presented as functions of satellite view angle or pixel position on scanline. Vegetative index simulations are also profiled.

17. Key Words (Suggested by Author(s))		18. Distribution Statement
Atmospheric aerosols	Vegetative index	
Radiation transfer	AVHRR	
Data simulation	Vegetative index number	
Metsat	NOAA6	
J. V. Dave dataset	NOAA7	

19. Security Classif. (of this report)	20. Security Classif. (of this page)	21. No. of Pages	22. Price*
Unclassified	Unclassified	33	

*For sale by the National Technical Information Service, Springfield, Virginia 22161

EW-L2-04387
JSC-18589

ATMOSPHERIC EFFECTS ON METSAT DATA

Job Order 72-456

This report describes activities of the Early Warning/Crop Condition Assessment project of the AgRISTARS program.

PREPARED BY

W. R. Johnson

APPROVED BY

USDA

G. O. Boatwright, Manager
Early Warning/Crop Condition
Assessment project, AgRISTARS
program

Lockheed-EMSCO

R. F. Hansen, Project Manager
Early Warning/Crop Condition
Assessment project, Inventory
Technology Development Department

LOCKHEED ENGINEERING AND MANAGEMENT SERVICES COMPANY, INC.

Under Contract NAS 9-15800

For

Earth Resources Applications Division

Space and Life Sciences Directorate

NATIONAL AERONAUTICS AND SPACE ADMINISTRATION
LYNDON B. JOHNSON SPACE CENTER
HOUSTON, TEXAS

January 1983

LEMSCO-18836

PREFACE

The Agriculture and Resources Inventory Surveys Through Aerospace Remote Sensing (AgRISTARS) program is a multiyear program of research, development, evaluation, and application of aerospace remote sensing for agricultural resources, which began in 1980. This program is a cooperative effort of the U.S. Department of Agriculture, National Aeronautics and Space Administration, National Oceanic and Atmospheric Administration (U.S. Department of Commerce), Agency for International Development (U.S. Department of State), and U.S. Department of the Interior.

ii, iii, iv

CONTENTS

TABLES

FIGURES

ACRONYMS

AgRISTARS	Agriculture and Resources Inventory Surveys Through Aerospace Remote Sensing
AVHRR	Advanced very high resolution radiometer
GMI	Gray McCrary index
Metsat	Meteorological satellites
NOAA	National Oceanic and Atmospheric Administration
VIN	Vegetative index number

1. INTRODUCTION

Scientists of the Early Warning project[1] are investigating the effects induced upon NOAA6 and NOAA7 advanced very high resolution radiometer (AVHRR) satellite data by an increasingly thick atmosphere, as the scanner view angle reaches on the periphery of the scan. [National Oceanic and Atmospheric Administration (NOAA) is a division of the U.S. Department of Commerce.] The effect of variable amounts of aerosols in the atmosphere also must be considered.

For this investigation, J. V. Dave provided an extensive dataset (ref. 1). He defines five different atmospheric models which are used to simulate direct solar radiation and diffuse radiation. The models represent a cloud free mid-latitude summer terrestrial atmosphere. The models considered vary from one with no absorption of aerosols to one with large amounts of absorption. A summary of the Dave dataset is provided in table 1-1, giving information on all five models.

According to Dave, "The atmospheric model is assumed to rest on a surface obeying Lamberts law of reflection. A fraction of the total energy incident on a Lambert surface is isotropically reflected by it, independent of the direction and the state of polarization of the incident radiation. Radiation reflected by a Lambert surface is unpolarized." Since some of the Earth surface is non-isotropic and does not always conform to Lambertian characteristics, some of the results derived here should be used with discretion.

The radiation data generated by these J. V. Dave models are stored on magnetic tape, providing information on the spectral, directional, altitudinal, and solar position dependence of the solar energy scattered by plane-parallel atmospheric models.

[1]A project of the Agriculture and Resources Inventory Surveys Thorough Aerospace Remote Sensing (AgRISTARS) program.

TABLE 1-1.- J. V. DAVE DATASET DESCRIPTION

(a)

Number of models	Number of computer tapes for each model	Total number of computer tapes
5	5 (Data at 60 km, 3 km, 2 km, 1 km, and at surface)	25

(b)

Information for each model

Seven Sun angles, incident at 0°, 30°, 45°, 60°, 70°, 75°, and 80°

Intensity of diffuse radiation provided for:

34 azimuth angles

2J upward vertical angles

- At five levels of atmosphere
- At 77 wavelength intervals of solar spectrum from 0.305 to 2.5 micrometers.

(c)

A cloud free midlatitude summer terrestrial atmosphere			
Model number	Gaseous absorption[a]	Number of aerosol particles in column, 1 cm^2 cross section	Size distribution function of aerosols
1	No	0	-
2	Yes	0	-
3	Yes	19.815×10^6	haze L
4	Yes	99.075×10^6	haze L
5	Yes	4.673×10^6	haze M

[a]Gaseous absorption includes water vapor (2.96 gm cm^{-2}) and ozone (0.308 atm - cm) in 1 cm^2 atmospheric cross section.

Three of Dave's models are ideally suited to simulate data recorded by bands 1 and 2 of the AVHRR aboard NOAA6 and NOAA7 meteorological satellites. These satellites have a near-polar orbit of the Earth at 833 kilometers altitude (ref. 2). Models 2, 3, and 4 have the normal atmospheric gaseous constituents plus the absorbing gases of ozone and water vapor (surface pressure = 1013 mbs; total ozone = 0.308 atm-cm; total water vapor content = 2.96 gm cm^{-2}). Model 2 has no aerosol; model 3 has aerosol content whose optical thickness at 0.6 microns is 0.09, and model 4 has aerosol content whose optical thickness at 0.6 microns is 0.45.

It should be noted that the Dave models simulate only a part of the problem of radiation through an atmosphere. The latitude and longitude variation in the amounts of the absorbing gases, especially water vapor and ozone, is quite large and affects the transmittance through the atmosphere. A similar variation in the amount of other particulates, such as invisible water droplets and/or ice crystals, also affects radiance recorded by satellite systems. Unfortunately, solutions of radiation transfer through atmospheres with the above mentioned constituent variations have not prompted new datasets.

The AVHRR data swath covers approximately 2925 kilometers, scanning from 55.4° right to 55.4° left of the ground track. Because of the Earth's curvature, these extreme zenith angles become 68.55° for Earth-bound observers looking at the satellite; see figure 1-1. The Sun incident angle will vary 26° when the scanline is aligned with the solar plane.

The Dave dataset provides data at zenith (surface to satellite) look angles of 0°, 10°, 20°, 30°, 40°, 50°, 60°, 65°, and 70°; at solar incident angles of 0°, 30°, 45°, 60°, 70°, 75°; and 34 delazimuth angles. (Delazimuth angles are the azimuth angle difference between the Metsat scanline direction and the direction of the Sun from the Metsat nadir vector.)

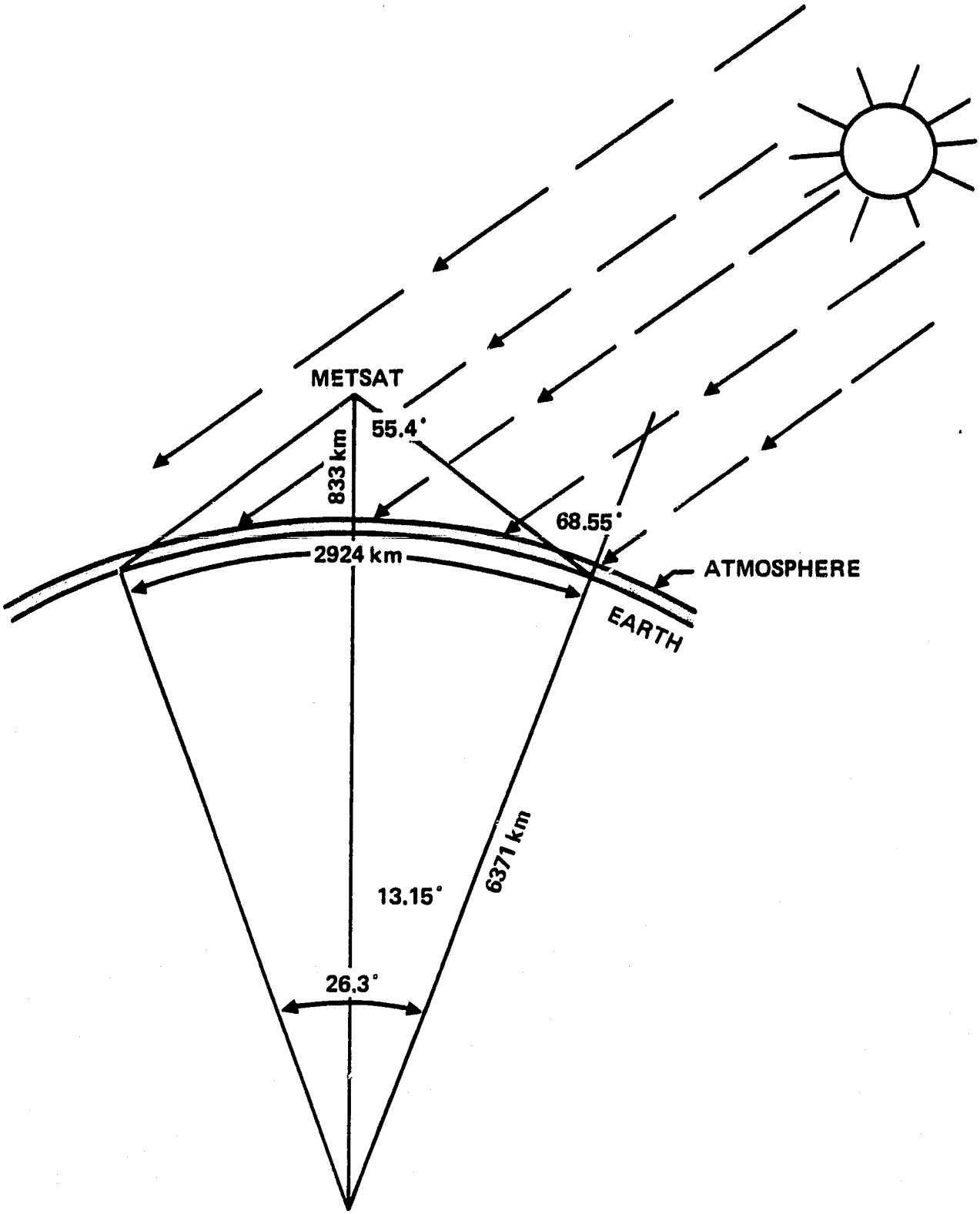

Figure 1-1.- Geometry of METSAT on Earth.

2. PROGRAM DESIGN

Software entitled METCOR4 was developed to generate radiance profiles portraying the atmosphere effect on the Metsat AVHRR data in the 111° swath. Operationally, given the solar zenith angle and the solar delazimuth angle, the software extracts pertinent information from the Dave dataset at each of nine wavelength intervals comprising AVHRR band 1 and thirteen wavelength intervals comprising AVHRR band 2. The satellite transmission characteristics of each wavelength interval are applied, and results are summed to represent full AVHRR and response. Surface reflectances of 0, 0.15, and 0.30 (arbitrarily assigned) of the incident energy at the surface are applied at each of the look angles from the surface to satellite with reference to selected delazimuth angles of 0°, 30°, 60°, and 90°. An algorithm developed by J. F. Potter* was used to process the extracted radiance data at the top and bottom of the atmosphere (see appendix A).

Executing METCOR4 with each model (with different aerosol concentrations) provides data files of the AVHRR bands 1 and 2 data. Simulated scanline profiles of radiance at the specified surface reflectance, solar zenith angles, and delazimuth angles are subsequently plotted.

*Private correspondence and papers of J. F. Potter, 1981, Lockheed Engineering and Management Services Company, Inc.

3. DISCUSSION OF PLOTS REPRESENTING RADIANCES RECORDED BY METSAT'S AVHRR

The profiles of the radiance have been plotted as a function of the 2048 pixels in the Metsat AVHRR scanline. Those plots which are related to NOAA6 and NOAA7 satellites are prepared to represent solar zenith angles and delazimuth angles that are usually encountered. Since NOAA6 passes the equator southbound at about 7:40 a.m. local time, most of the solar zenith angles at nadir will be between 45° and 60°, with the Sun to the east (U.S. viewing), resulting in the delazimuth angle being near zero. Thus, with sensor scanning from right to left, the pixel number increases eastward toward the Sun.

NOAA 7 passes the equator northbound about 1:30 p.m. local time such that the solar zenith angles at nadir are between 0° and 30°; the delazimuth angle is near 50°, with the Sun being to the south-southwest. Here again with the sensor scanning right to left, the higher pixel numbers will be aligned about 60° off the direction of the Sun.

Figures 3-1 and 3-2 represent NOAA6 AVHRR band 1 radiances as would be observed with solar zenith angles of 45° and 60°, respectively. Each figure consists of three plots portraying profiles as though the entire area along scanline had surface reflectance of 0°, 0.15°, and 0.30°. The three profiles in a plot represent an atmosphere with the three levels of aerosols defined on the plots as aerosal optical depth, tau. Figures 3-3 and 3-4 are data for NOAA6 AVHRR band 2. Figures 3-5 and 3-6 represent NOAA7 AVHRR band 1 radiances as should be observed with solar zenith angles of 0° and 30°, respectively. Profiles are the same as in figure 3-1. Figure 3-7 represents data as presented in figure 3-5, except the data are for NOAA7 AVHRR band 2.

The radiance values are in milliwatts/cm^2-micron-steradian. These values are converted to albedo counts, a linear function of the digital AVHRR radiometer count. (Calibration procedures are discussed in later paragraphs.) The albedo counts are provided on the right side of the plots and agree realistically with observed values from the satellite. M. J. Duggin et al. (ref. 3) analyzed

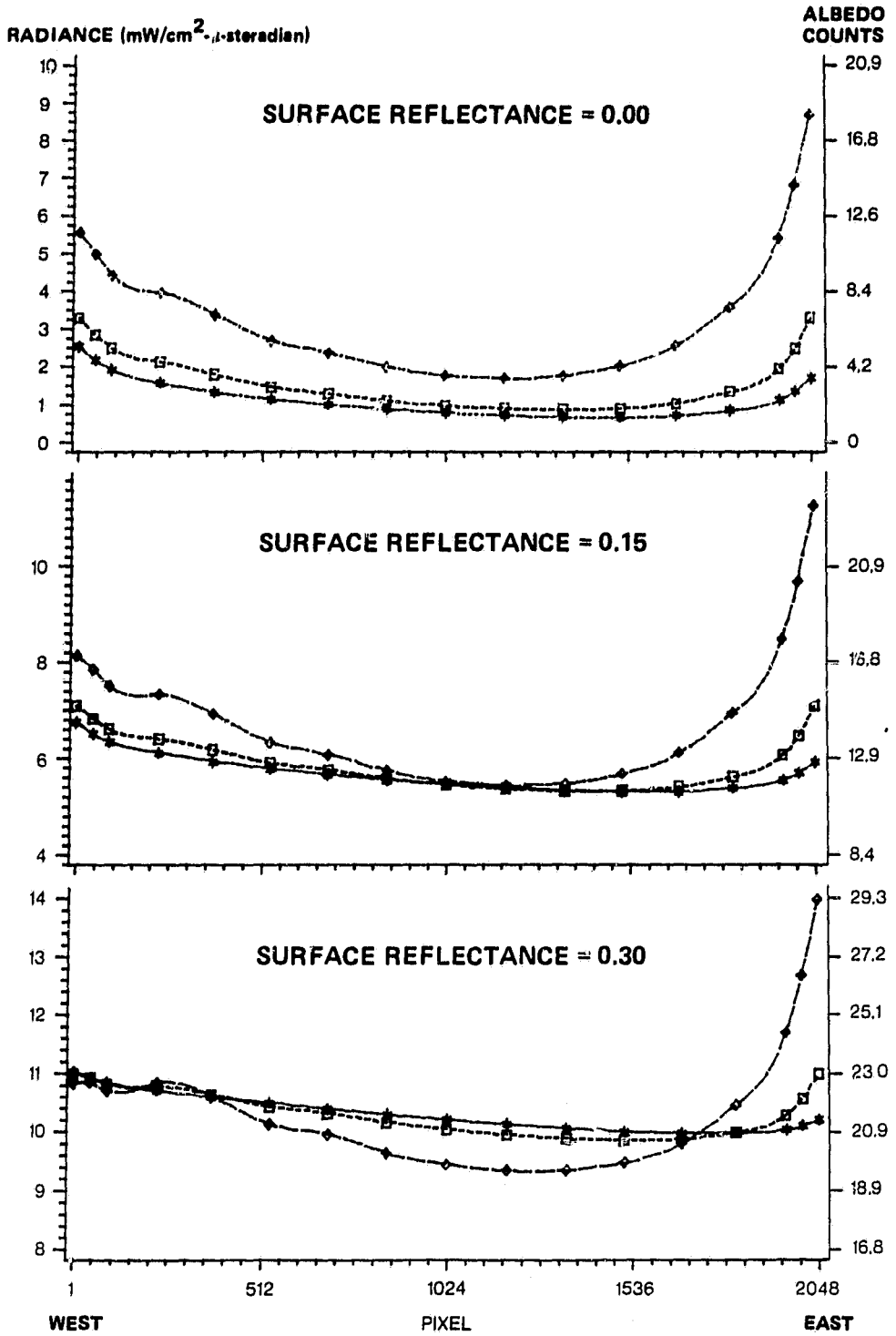

Figure 3-1.- NOAA6 AVHRR band 1 atmospheric effects as observed with solar zenith angle of 45° and the reflectance = 0.00, 0.15, and 0.30.

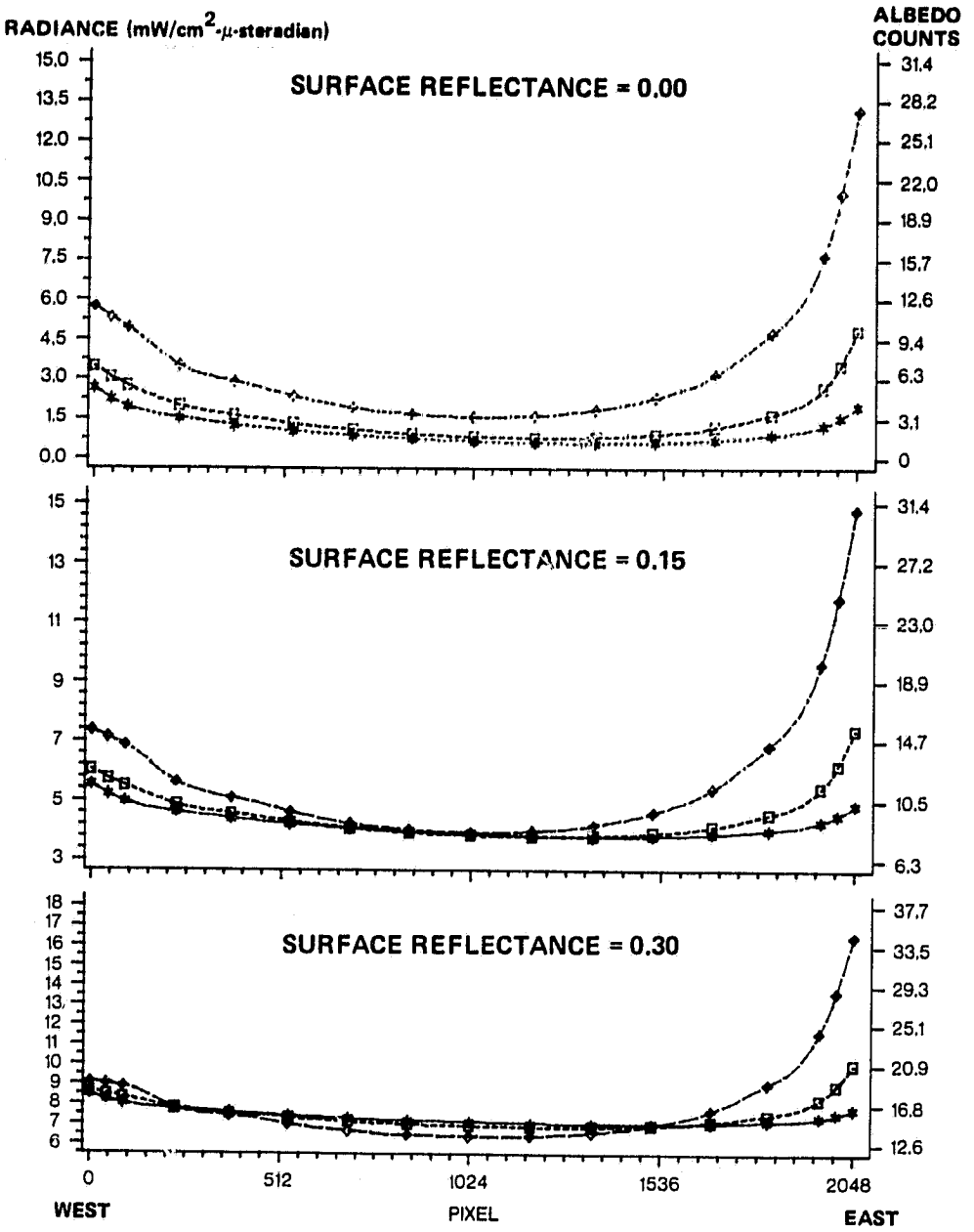

Figure 3-2.- NOAA6 AVHRR band 1 atmospheric effects as observed with solar zenith angle of 60° and the reflectance = 0.00, 0.15, and 0.30.

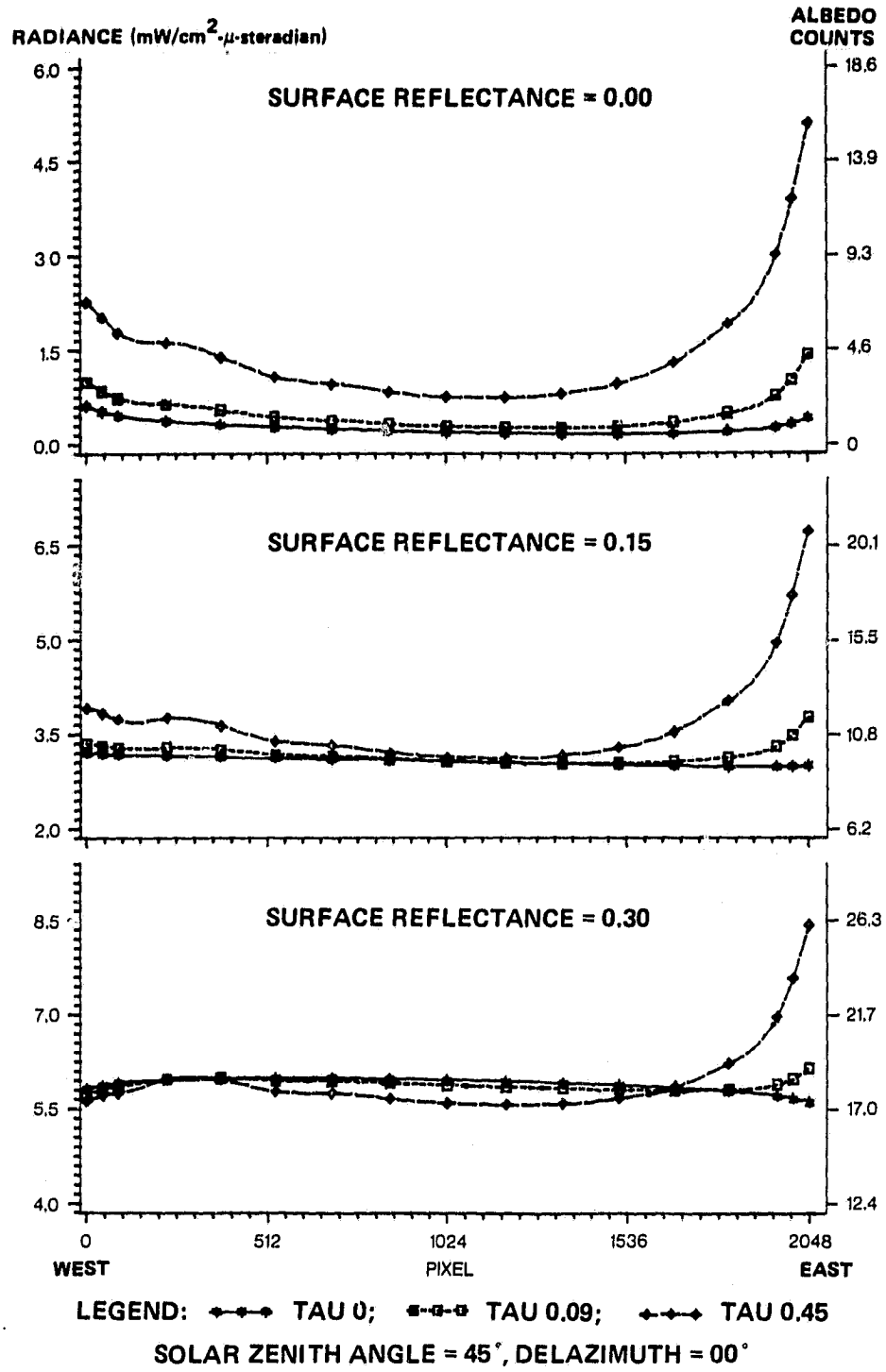

Figure 3-3.- NOAA6 AVHRR band 2 atmospheric effects as observed with solar zenith angle of 45° and the reflectance = 0.00, 0.15, and 0.30.

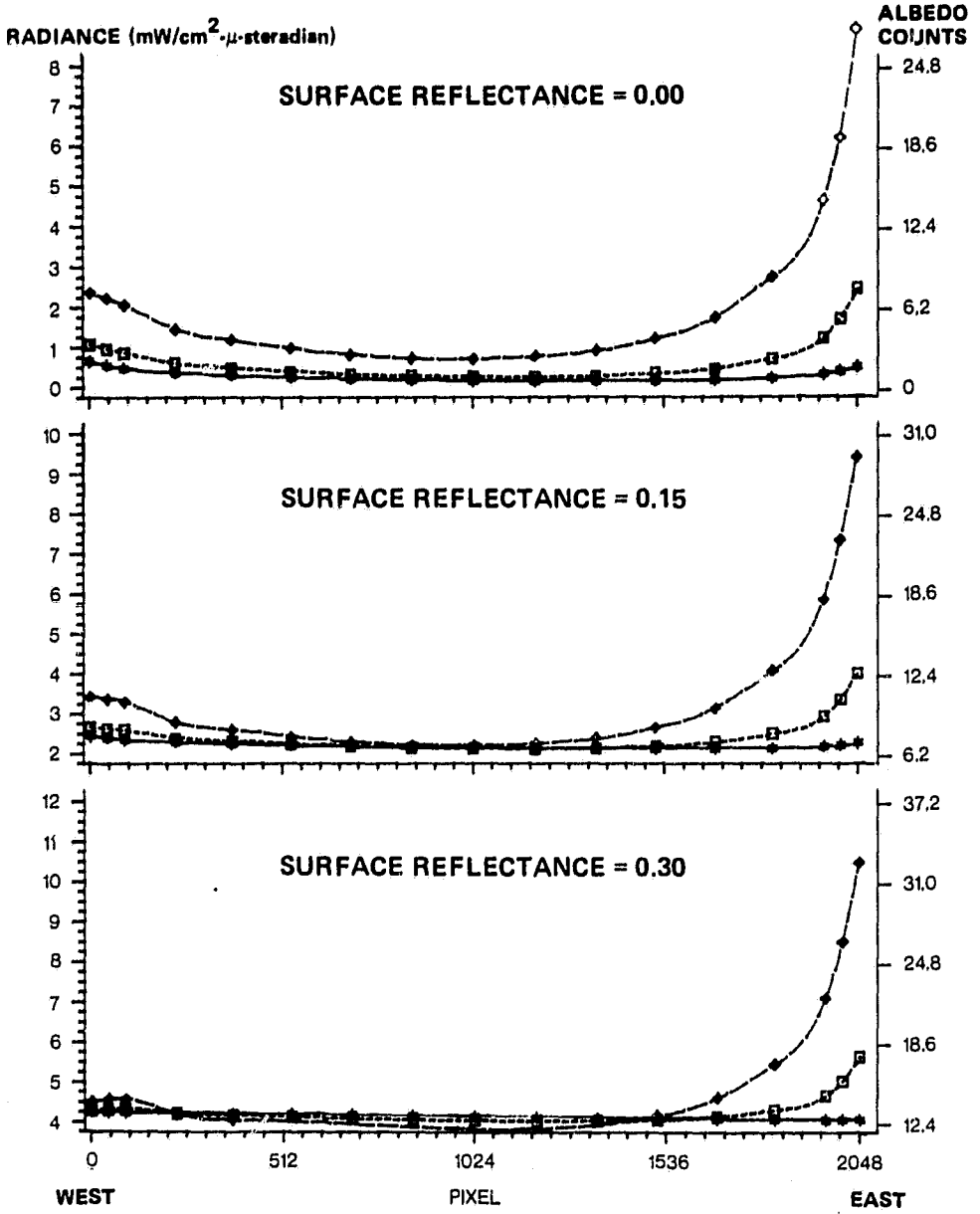

Figure 3-4.- NOAA6 AVHRR band 2 atmospheric effects as observed with solar zenith angle of 60° and the reflectance = 0.00, 0.15, 0.30.

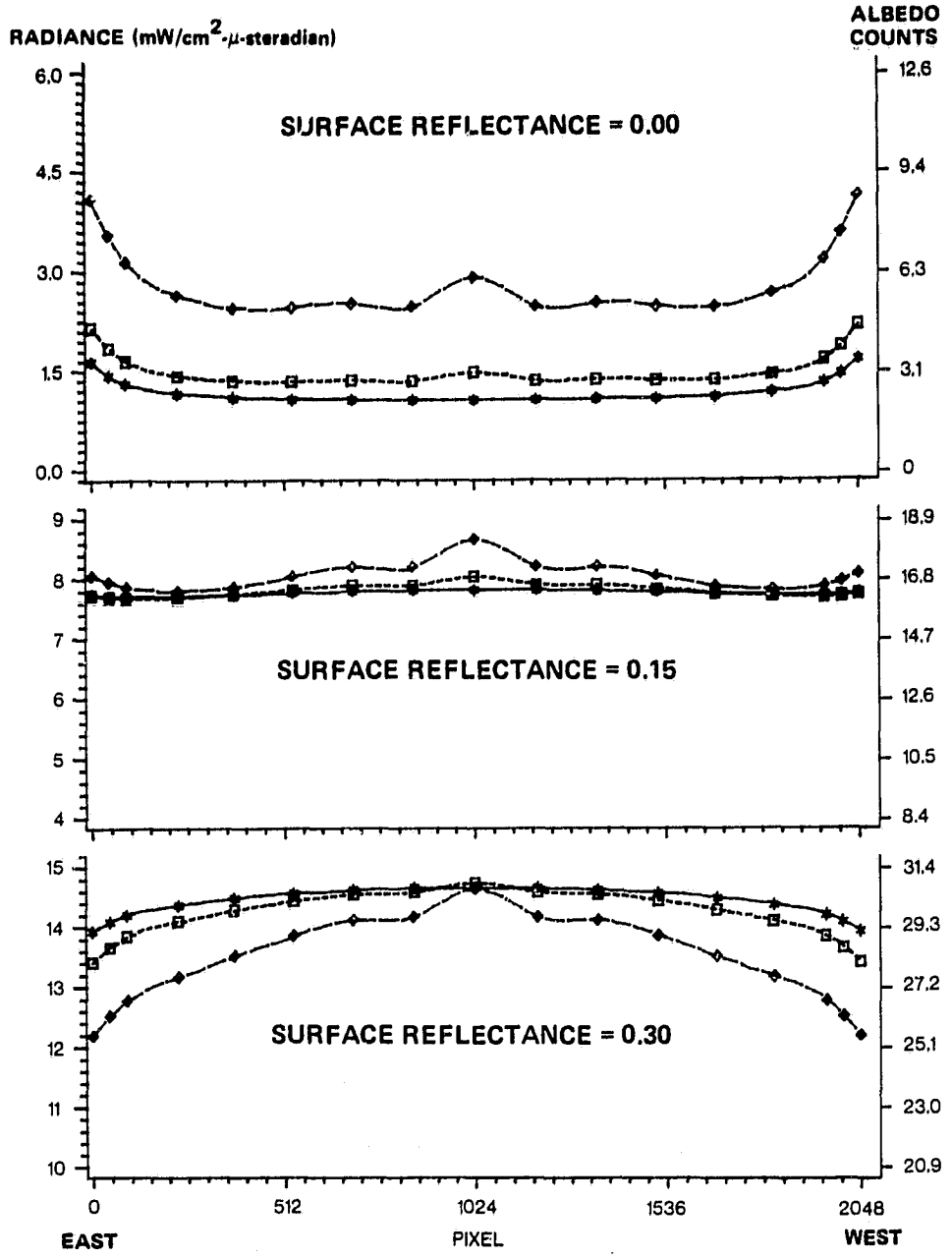

Figure 3-5.- NOAA7 AVHRR band 1 atmospheric effects as observed with solar zenith angle of 0° and the reflectance = 0.00, 0.15, and 0.30.

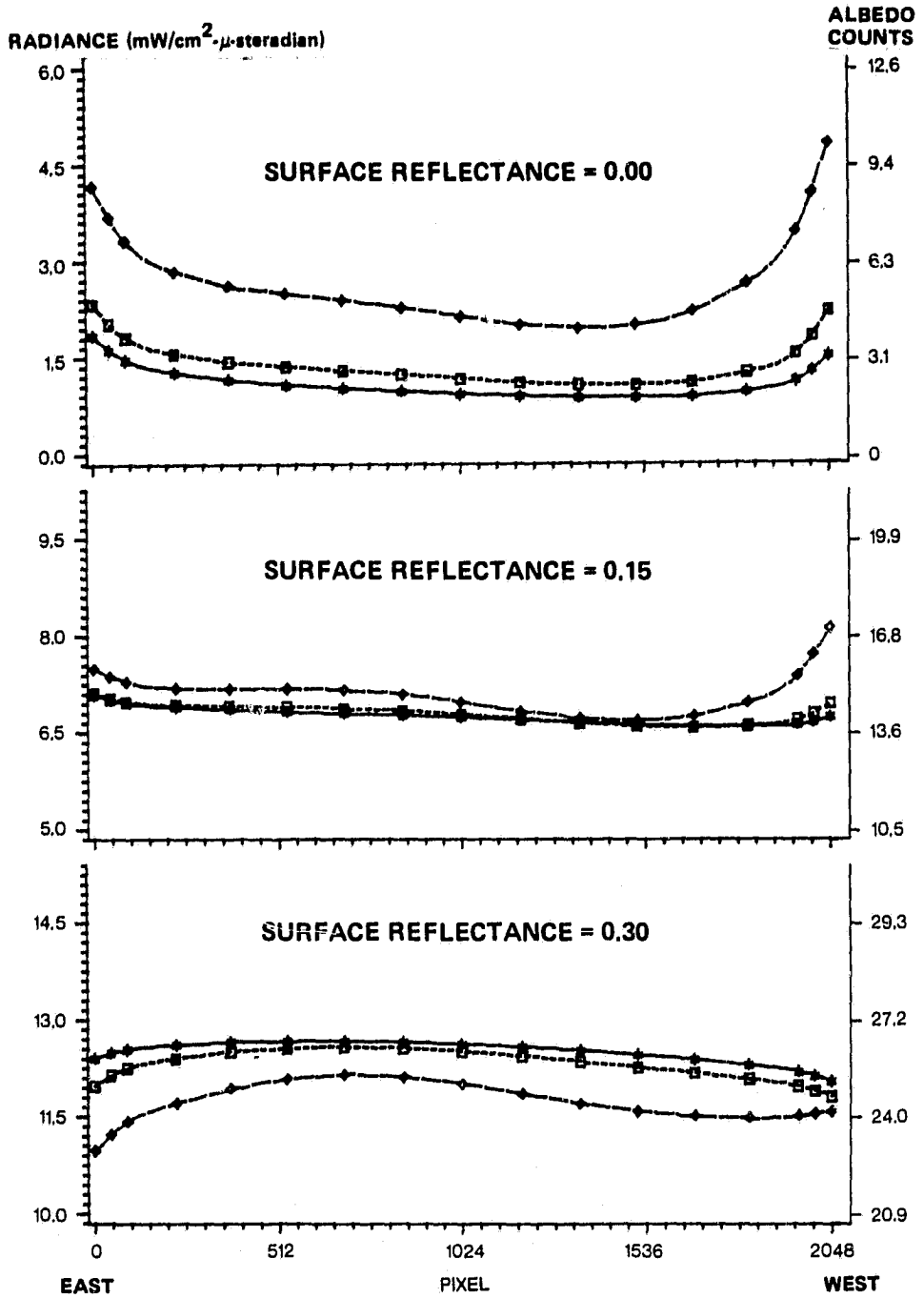

Figure 3-6.- NOAA7 AVHRR band 1 atmospheric effects as observed with solar zenith angle of 30° and the reflectance = 0.00, 0.15, and 0.30.

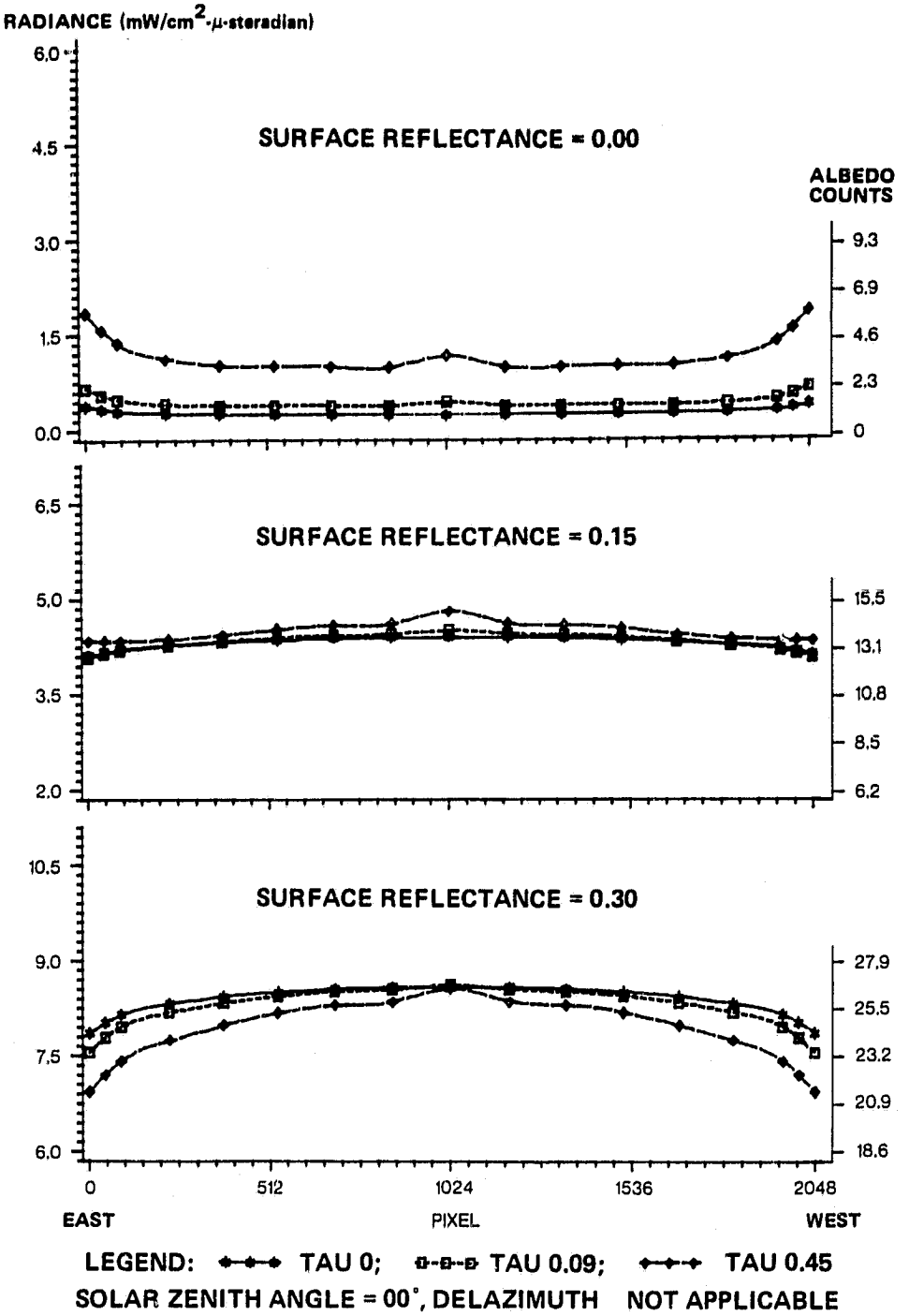

Figure 3-7.- NOAA7 AVHRR band 2 atmospheric effects as observed with solar zenith angle of 0° and the reflectance = 0.00, 0.15, and 0.30.

100 sequential lines of NOAA6 AVHRR data, scanning a relatively cloud free area on Julian day 169 in 1980. Averaged pixels in each 5-pixel interval along the scanline for these scanlines are shown in figure 3-8, and the characteristic higher radiance at each end of the scanline is also shown.

The plots were prepared to show the significance of aerosol concentrations at a specified surface reflectance. A series of these plots with different reflectances demonstrate the significance of the location of the reflecting surface on a scanline.

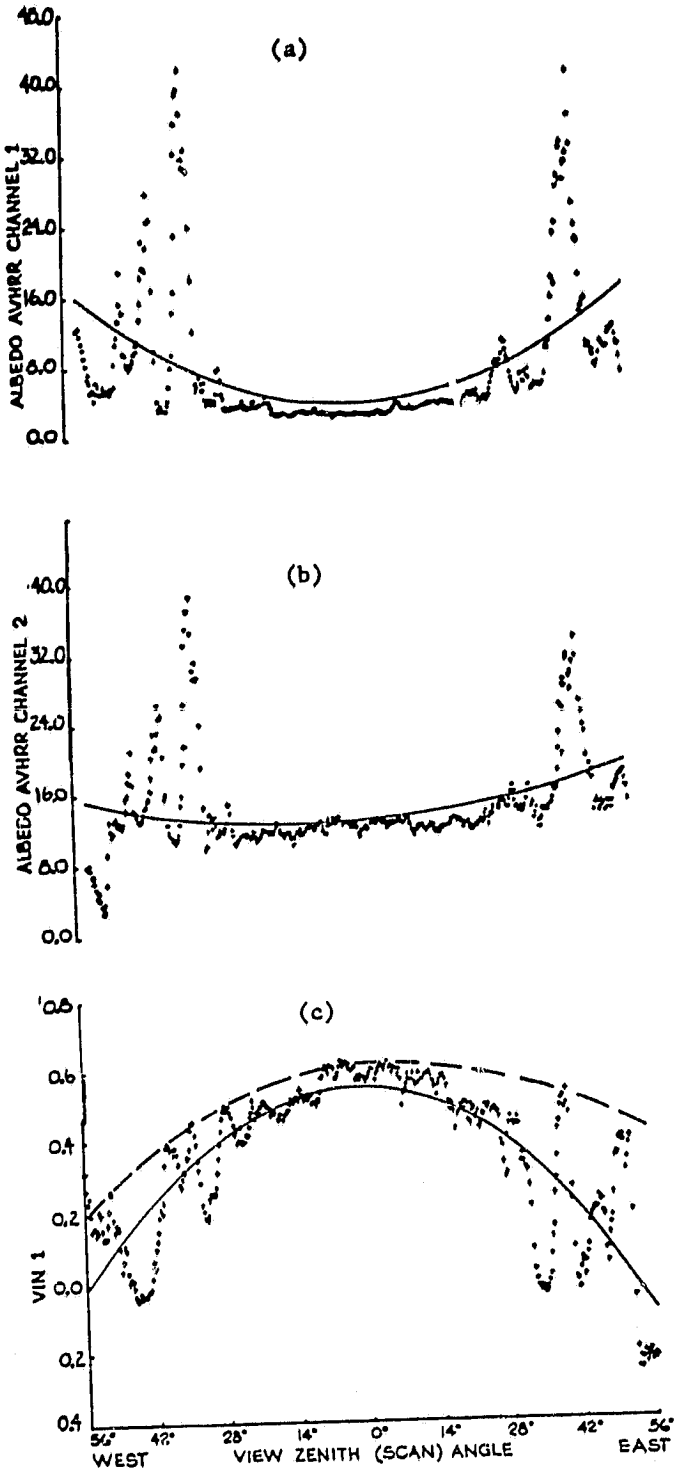

Figure 3-8.- Observed NOAA6 AVHRR sensor output and vegetative index (normalized difference of sensor outputs) shown as a function of view zenith (scan) angle (ref. 3).

4. DATA CONVERSION

The results of the processing with METCOR4 provide results in units of milliwatts/cm^2-micron-steradian and millwatts/cm^2-steradian. Most application requires analysis of Metsat data to be done in albedo counts which are derived from the AVHRR imagery data. The NOAA6 and NOAA7 AVHRR instruments were calibrated using a 30-inch spherical integrator consisting of 12 lamps (ref. 4). The integrating sphere calibration was done in November 1974; it was rechecked in November 1978 shortly after NOAA6 and NOAA7 AVHRR instruments were calibrated and found to have changed less that 2 percent, well within the calibration accuracy desired*. With a profile of the spectral radiant emittance of the spherical integrator versus wavelength and with the individual Metsat band transmission response curves, the irradiances for each band were calculated and associated with a published percent albedo. The results of these calculations are in table 4-1. These values permit conversion of the METCOR4 results from milliwatts/cm^2 steradian to albedo counts which are given in table 4-2.

TABLE 4-1.- METSAT AVHRR CONVERSION PARAMETERS

Metsat AVHRR	Spectral width, microns	Spherical integrator irradiance, mW/cm^2 steradian	Albedo, percent	Conversion factor, albedo to mW
Band 1	0.58 to 0.68	37.773	79.1	0.4775
Band 2	0.713 to .986	30.004	93.13	0.3225

*Correspondence of A. W. McCullock in 1982, NASA at Goddard Space Center, Greenbelt, Maryland.

TABLE 4-2.- CONVERSION FROM MILLIWATTS/cm^2 STERADIAN TO AVHRR ALBEDO COUNTS

Milliwatts	Band 1, $albedo_1$	Band 2, $albedo_2$
1	2.1	3.1
2	4.2	6.2
3	6.3	9.3
4	8.4	12.4
5	10.5	15.5
6	12.6	18.6
7	14.7	21.7
8	16.8	24.8
9	18.9	27.9
10	20.9	31.0
11	23.0	34.1
12	25.1	37.2
13	27.2	40.3
14	29.3	43.4
15	31.4	46.5
16	33.5	49.6
17	35.6	52.7

Channel 1: $albedo_1 = mW_1/0.4775$

Channel 2: $albedo_2 = mW_2/0.3225$

Satellite data:

Channel 1: $0.1071 \times counts_1 - 4.11 = albedo_1$

Channel 2: $0.1058 \times counts_2 - 3.45 = albedo_2$

5. GRAY-McCRARY INDEX (GMI) SIMULATION

Vegetative signatures are usually recognized when band 2 reflectance exceeds band 1 reflectance by 0.15 or more. By using the profile data in section 3, samples of vegetative indices can be computed and profiled. The Gray-McCrary index [also known as the environmental vegetative index and vegetation index number (VIN)] is defined as band 2 albedo count minus band 1 albedo count. GMI values are being studied to relate their values to the vegetation growth and stress cycles. Figure 5-1 represents GMI profiles as would be expected from NOAA6 AVHRR data recorded in the three different atmospheres with differing aerosol optical depths, tau = 0, 0.09, and 0.45, respectively. The figure consists of 3 plots; each plot consist of two sets of curves; each set represents two solar incident angles of 45° and 60° at the specified band 2 minus band 1 reflectance difference (channel 2 reflectance minus channel 1 reflectance). Figure 5-2 represents profiles as would be determined from the NOAA7 AVHRR data.

The profile is not unlike that which is portrayed in figure 3-8 (c), section 3. The curve in figure 3-8 (c) has been normalized[a]; however, the shape of the profile of the unnormalized curve with different ordinate values has been shown to be similar to that of the GMI curve.

Comparison of these profiles to profiles of real data should consider changes in the Sun incident angles along the profile. In using the simulated NOAA6 data (fig. 5-1), a gradual shift from the lower set of curves to the top set is made as one progresses along the scanline pixels. This same characteristic can be followed in the dashed curve of figure 3-8 (c).

---

[a](band 2 albedo - band 1 albedo)/(band 2 albedo + band 1 albedo)

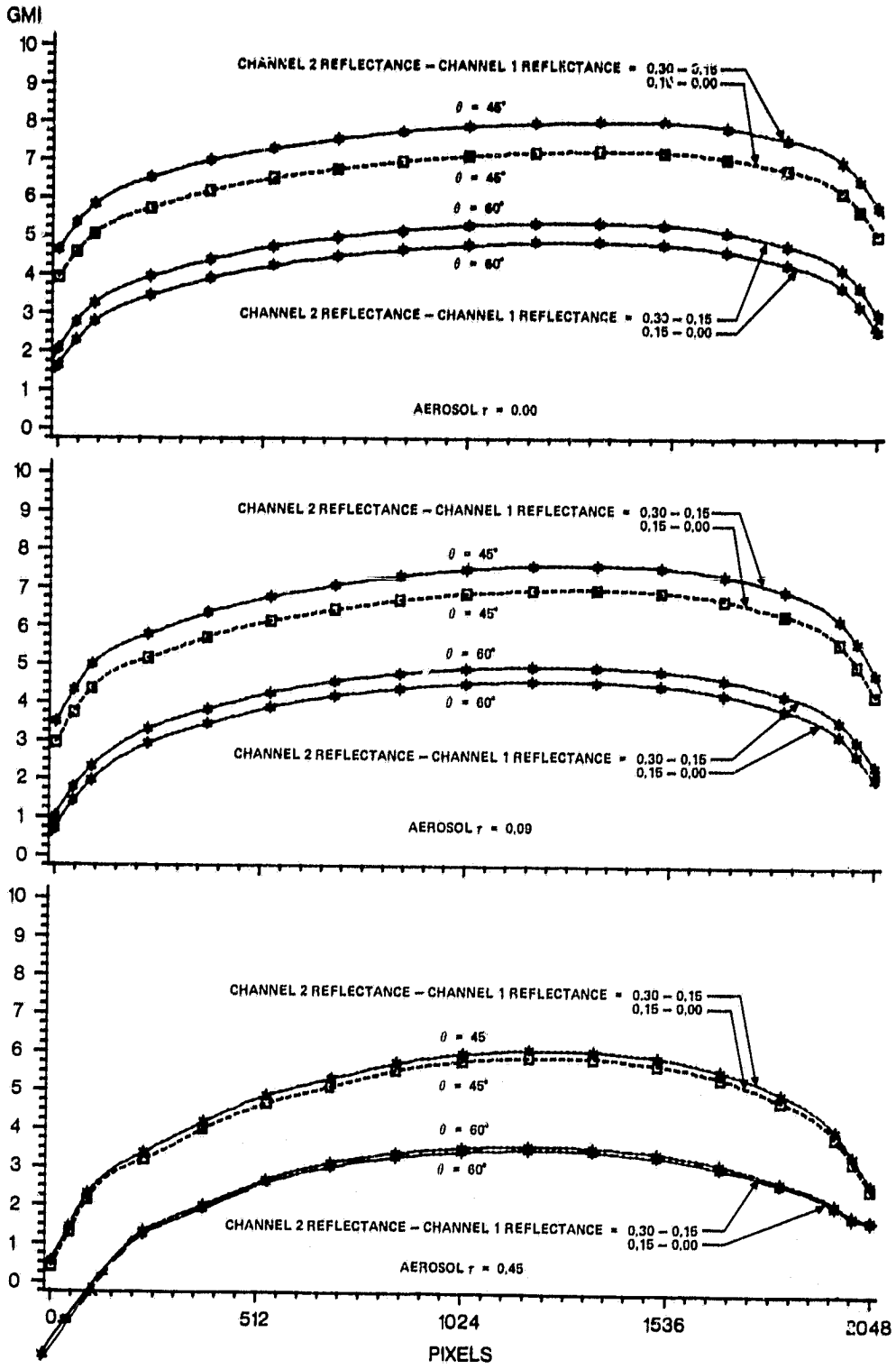

Figure 5-1.- NOAA6 plots of GMI versus pixel on scanline at two values of Sun incident angle Θ and two values of channel 2 reflectance minus channel 1 reflectance, azimuth angle = 0°.

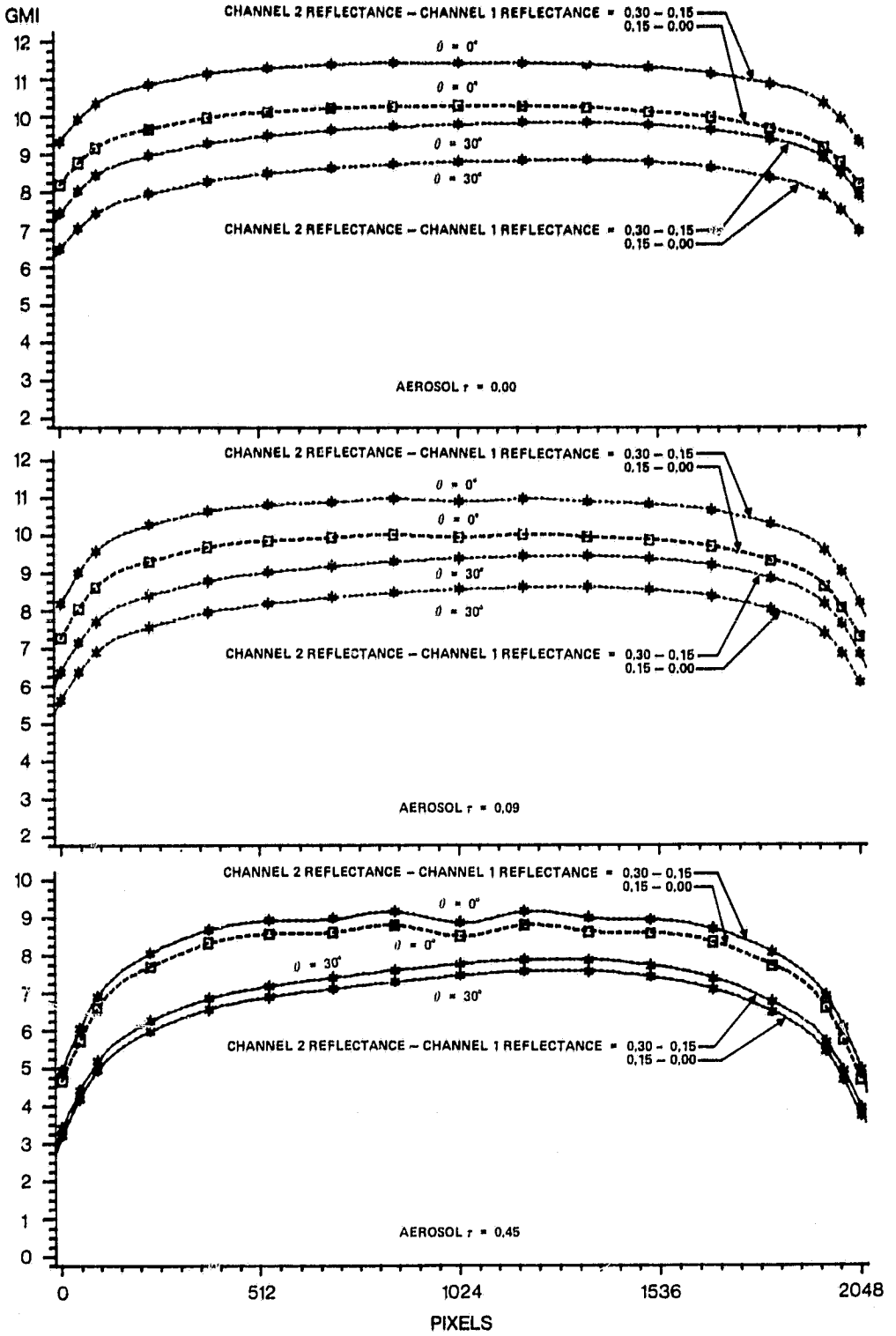

Figure 5-2.- NOAA7 plots of GMI versus pixels on scanline at two values of Sun incident angle Θ and two values of channel 2 reflectance minus channel 1 reflectance, azimuth angle = 60°.

6. CONCLUSIONS

Satellite data simulations have been successful using the Dave dataset involving three atmospheric models which have fixed amounts of absorbing gases with variable amounts of aerosols. The results appear valid. Comparison of the simulated data with actual AVHRR data acquired in the cloud free regions in central United States is good. Precise comparison is not possible, since precise aerosol content of the atmosphere nor the regional spectral reflectances are known when the AVHRR data are acquired. However, best estimates of both aerosol optical depths and surface reflectance applied to the data simulations show good agreement. Results of these simulations of the AVHRR data offer opportunities to evaluate the observed data in light of the expected variations of aerosols in the atmosphere along the 2,900-kilometer path of the scanline. Future atmospheric models, which will vary the amount of the absorbing gases and the inclusion of water and ice particles in the ray path, will permit an extension of this evaluation. The status of development of these future models is not known.

These series of radiance/count plots are useful in estimating limits of data which can be expected on an AVHRR scanline, knowing the solar incident angle and the temporal continuity of reflectance from the targeted scene. In some cases at the extreme end of the scanline toward the Sun, the influence of an aerosol concentration on the data can be seen, and perhaps it can be used as an estimator of aerosol concentration. In most cases, for a target with known reflectance, variation of three or less albedo counts on the scanline can be attributed to an aerosol variation of 0.45 optical depth. If one were confident that there are no changes in absorbing gas quantities nor water-ice particles along the scanline, variation of three albedo counts could be significant. However, at this time the three albedo counts will be considered as noise. The plotted data do provide guidance to utilize more of the data on the scanline. Currently, data analysts, in their crop assessment operations, have restricted data to be within 256 pixels of nadir to assure that look angle effects do not distort the data. These graphs suggest that data on a scanline can be extended to twice this span of data.

The series of GMI plots show a repetitious profile along the scanline where GMI value becomes a function of: (a) solar illumination, (b) the difference between the channel reflectances, and (c) the aerosol concentration. The GMI increases with decreasing solar zenith angle; the GMI decreases with increasing aerosol concentration; and the GMI increases with increasing channel 2 and channel 1 differences in surface reflectances. Figures 5-1 and 5-2 in section 5 show the profiles illustrating each of the above GMI influences.

Based on the processed NOAA AVHRR data and the available information on the Earth's surface, Dave's data set is considered a good instrument to pursue analysis of data from satellite systems.

The profiles presented in section 3 indicate that the solar zenith angle is an important factor in determining when the atmosphere begins to adversely affect the data from satellites viewing at large angle from nadir. For NOAA6, viewing at low Sun elevation angles, the data variation is relatively good until scan reaches 30° from nadir. For NOAA7, viewing at high Sun elevation angles, the same data variation can be expected when the scan reaches 40° or 50° from nadir. In both cases, the position of Sun, with respect to the satellite view, should be considered.

By use of the Dave dataset, simulated spectral data from the satellite radiometric systems can prepare data analysts to consider the geometry of insolation and satellite viewing in their operations. Until techniques are developed to probe the atmosphere to acquire optical depth values due to aerosols and other gaseous constituents, satellite data analysts must live with an error in recorded radiance. This study begins to show what error can be expected due to some aerosols and the satellite-viewing angle.

7. REFERENCES

1. Dave, J. V.: Extensive Datasets of the Diffuse Radiation in Realistic Atmosphere Models with Aerosols and Common Absorbing Gases. Solar Energy, Vol. 21, 1978, pp. 361-369.

2. Kidwell, K. B.: NOAA Polar Orbiter Data, Users Guide. U.S. Department of Commerce, Washington D.C., 1981.

3. Duggin, M. J.; Piwinski, D.; Whitehead, V.; and Ryland, E.: Evaluation of NOAA-AVHRR Data for Crop Assessment. Applied Optics, Vol. 21, No. 11, 1982, pp. 1873-75.

4. Alignment and Calibration Data Book, AVHRR/2, PFM. Indiana Institute of Technology, Ft. Wayne, Indiana, 1974.

APPENDIX A

ALGORITHM OF DR. J. F. POTTER

APPENDIX A

ALGORITHM OF DR. J. F. POTTER

In term of Dave's data set documentation for a specified atmospheric model, solar zenith angle, and wavelength, the following algorithm was developed.

$$I(\theta,\phi,R,R^1) = \varepsilon I(\theta,\phi) + \varepsilon IST(\theta) \times \frac{R}{1-R\bar{S}} + \left(\frac{R-R^1}{1-R\bar{S}}\right)$$

$$\times \text{GRND} \times \exp(-\text{DTAUBS} \times \sec\theta)$$

where

θ = Zenith angle of the direction of diffuse radiation

ϕ = Azimuth angle; angle which the vertical plan containing direction of the diffuse radiation makes with the Sun's meridian

R = Reflectivity of Lambert ground outside scanner field of view

R^1 = Reflectivity of Lambert target within scanner field of view

I = Observed radiance (intensity)

EI = Intensity of diffuse radiation at 60 km

EIST = Intensity of reflected energy at 60 km; to be added to EI for including the effect of Lambert ground of reflectivity R at lower boundary

GRND = Intensity at 0.0 km; Lambert ground reflection contribution to the scattered radiation

$\bar{S}$ = Diffuse flux reflectivity of model for case of isotropic illumination

DTAUBS = Total Optical depth of model atmosphere.

NOTE

All calculations performed in this study consider $R = R^1$, thus, reducing equation to first two terms.